Biochemical and Biophysical Research Communications 401 (2010) 131–136

Contents lists available at ScienceDirect

Biochemical and Biophysical Research Communications

journal homepage: www.elsevier.com/locate/ybbrc

Reduction of Nup107 attenuates the growth factor signaling in the senescent cells

Sung Young Kim, Hyun Tae Kang, Hae Ri Choi, Sang Chul Park *

Department of Biochemistry and Molecular Biology, Aging and Apoptosis Research Center, Seoul National University College of Medicine, Seoul 110-799, Republic of Korea

ARTICLE INFO

Article history:
Received 1 September 2010
Available online 15 September 2010

Keywords:
Nup107
Extracellular signal-regulated kinase
Senescence
Oligodendroglioma
Fibroblast

ABSTRACT

Hypo-responsiveness to growth factors is a fundamental feature of cellular senescence. In this study, we found markedly decreased level of Nup107, a key scaffold protein in nuclear pore complex assembly, in senescent human diploid fibroblasts as well as in organs of aged mice. Depletion of Nup107 by specific siRNA in young human diploid fibroblasts prevented the effective nuclear translocation of phosphorylated extracellular signal-regulated kinase (ERK) following epidermal growth factor (EGF) stimulation, and decreased the expression of c-Fos in consequence. The disturbances in ERK signaling in Nup107 depleted cells closely mirror the similar changes in senescent cells. Knockdown of Nup107 in anaplastic oligodendroglioma cells caused cell death, rather than growth retardation, indicating a greater sensitivity to Nup107 depletion in cancer cells than in normal cells. These findings support the notion that Nup107 may contribute significantly to the regulation of cell fate in aged and transformed cells by modulating nuclear trafficking of signal molecules.

1. Introduction

An age-related decline in growth factor signaling is one of the characteristic features of senescent cells. For example, ERK signaling is perturbed in senescent cells and Elk-1 phosphorylation as a result of activation of ERK signaling is necessary for c-Fos gene activation [1–5]. Previous studies have demonstrated that senescent cells show the impaired phosphorylation of Elk-1 in response to epidermal growth factor (EGF) [6] and dysfunctional induction of c-Fos upon exposure to stimuli, including serum [7], mitogenic growth factors [7], and antioxidants [8]. Despite extensive researches, the mechanism underlying this decline remains poorly understood. Many signaling molecules, as well as transcription factors, perform their roles following their import to the nucleus. We previously showed that p-ERK1/2 accumulates in the cytoplasm and fails to translocate to the nucleus in senescent HDFs treated with EGF [9]. The lack of Elk-1 phosphorylation likely results from the reduced levels of active ERK proteins in the nuclei of senescent cells. However, the molecular mechanism for nuclear translocation of ERK has not been clarified yet. We have reported that the expression of genes involved in nucleocytoplasmic trafficking is suppressed in senescent cells to be compared with young cells [10]. From these results, we assumed the possible existence of aging-dependent functional barriers for the nucleocytoplasmic trafficking of signalings. In this context, we paid a special attention on the aging-dependent inefficiency of nuclear translocation of ERK signaling in response to EGF.

An earlier study has demonstrated that the scaffold protein Nup107 is essential for nuclear pore complex (NPC) assembly [11]. In its absence, nuclear membrane lacks formation of NPCs. Here, we examined the role of Nup107 in young and senescent HDFs and explored whether Nup107-related nuclear trafficking might be involved in aging-related attenuation of EGF signaling.

2. Materials and methods

2.1. Cell culture and transfection

Human diploid fibroblasts (HDFs) were isolated from the foreskin of a 6-year-old boy, healthy donor. Cells were grown in Dulbecco's modified eagle medium (DMEM) (Gibco BRL, Grand Island, NY, USA) containing 10% fetal bovine serum (FBS) (Gibco BRL, Grand Island, NY, USA) and 1% penicillin/streptomycin in a 5% CO_2 incubator. Cells were subcultured serially at a ratio of 1:4. We defined young cells as those resulting from <25 population doublings, and old cells were from >66 population doublings. SNU-738 human oligodendroglioma cells were purchased from the Korean Cell Line Bank (KCLB, Seoul, Korea). Cells were cultured in Dulbecco's modified eagle medium (DMEM) supplemented with 10% heat-inactivated FBS at 37 °C 5% CO_2 and 95% O_2 in a humidified cell incubator, and the medium was changed every 2–3 days. Cells were subcultured serially at a ratio of 1:3.

2.2. SA β-galactosidase staining

Cellular senescence of all of the old cells was confirmed by their delayed population doubling times (over 3 weeks) and by a

* Corresponding author. Fax: +82 2 744 4534.
E-mail address: scpark@snu.ac.kr (S.C. Park).

0006-291X/$ - see front matter © 2010 Elsevier Inc. All rights reserved.
doi:10.1016/j.bbrc.2010.09.025

senescence-associated β-galactosidase activity assay as described by Dimri et al. [12]. Cells were washed with phosphate-buffered saline and fixed with 2% paraformaldehyde containing 0.2% glutaraldehyde in phosphate-buffered saline for 5 min at room temperature. After washing with phosphate-buffered saline, cells were incubated with β-galactosidase reagent (1 mg/ml 5-bromo-4-chloro-3-indolyl-β-d-galactopyranoside (X-gal), 40 mm citric acid/sodium phosphate buffer, pH 6.0, 5 mm potassium ferrocyanide/potassium ferricyanide, 150 mm NaCl, 2 mm $MgCl_2$) at 37 °C.

2.3. Preparation of cytosol and nuclear extract

Subcellular fractionation was performed to prepare nuclear and cytosol extracts. Cells ($6 \times 10^{6)}$ were harvested by trypsin, washed three times with phosphate-buffered saline and resuspended to 6×10^6 cells/ml in TM-2 buffer containing 10 mM Tris, pH 7.4, 2 mM $MgCl_2$, 1 mM phenylmethylsulfonyl fluoride and protease inhibitors. Resuspended cells were incubated at room temperature for 1 min and then transferred into a tube in ice for 5 min with Triton X-100 added to a final concentration of 0.5% and incubated on ice for 10 min. Cell lysates were separated by 80 passages through a 26-gauge needle. The nuclei were isolated from the cytosol by centrifugation at 6000 rpm at 4 °C for 10 min. Isolated nuclei were washed with TM-2 buffer and resuspended in a nuclear extraction buffer containing 20 mM of Hepes, pH 7.9, 0.42 M NaCl, 1.5 mM $MgCl_2$, 25% (v/v) glycerol, 0.2 mM EDTA, 0.5 mM dithiothreitol and protease inhibitors. Resuspended nuclei were incubated on ice for 30 min with occasional shaking and sonicated to extract the nuclear proteins and finally were spun down in a microcentrifuge for 5 min.

2.4. Animals and homogenization of tissues

C57Bl/6 J male mice of two different age groups, young (4 months) and old (24 months), kept under standard laboratory conditions were used. The mice were killed by cervical dislocation. Lungs, livers, kidneys and intestine were frozen in liquid nitrogen and kept at −80 °C until further use. Frozen tissues were homogenized by 10–15 strokes each with a polytron tissue homogenizer and a Teflon glass homogenizer (GlasCol, Terre Haute, IN, USA) at high speed and sonicated with a VCX 400 sonication machine (Sonics & Materials Inc., CT, USA) in homogenization buffer (10 mM Tris–HCl, pH 7.6, 5 mM EDTA, 5 mM EGTA, 0.5 μg/ml antipain, 0.1 mM PMSF, 140 μg/ml trypsin inhibitor). The homogenate was centrifuged at 16,000×*g* for 15 min and the supernatant was collected and used in the subsequent experiments.

2.5. Western blotting and immunoprecipitation

Cells were lysed in a lysis buffer containing 50 mM Tris, pH 7.4, 150 mM NaCl, 1 mM EDTA, pH 8.0, 1 mM protease inhibitor cocktail (Roche), 1 mM phenylmethylsulphonyl fluoride (PMSF), 1 mM NaF, and 1 mM sodium orthovanadate. Protein samples were resolved by SDS–PAGE and transferred onto nitrocellulose membranes (Schleicher & Schuell Bioscience). The membranes were incubated with primary antibodies for 16 h at 4 °C and then with secondary antibodies for 1 h at RT. The antigen–antibody complexes were detected by enhanced chemiluminescence (Pierce). For immunoprecipitation cell lysates were gently mixed with specific antibodies and incubated overnight at 4 °C, followed by overnight incubation with protein A/magnetic beads (Milipore). The beads were washed three times with lysis buffer, eluted with SDS sample buffer and subjected to reducing SDS–PAGE. For reprobing, the membranes were stripped by incubation in 2% SDS, 100 mM β-mercaptoethanol, 62.5 mM Tris–HCl (pH 6.8) for 45 min at 50 °C. After extensive washing and blocking, the membranes were probed with the appropriate antibody and developed. Antibodies for actin (A5441), p-Erk (sc-7383) and p-Elk (sc-8406) were purchased from Santa Cruz Biotechnology. Antibodies for Nup107 (A301-9579) were purchased from Bethyl Laboratories. Quantitation of the band signals (from three independent experiments) was carried out by Gel-Pro analyzer version 3.1 (Media Cybernetics).

2.6. Immunofluorescence staining

Cells were plated on 24-well culture plates with coverslips and incubated with different stimuli for the indicated times. After incubation, cells were washed three times with ice-cold PBS and fixed in 4% paraformaldehyde/PBS for 15 min at room temperature, briefly washed in PBS, and permeabilized with 0.5% Triton X-100 in PBS for 10 min. After brief washing, cells were blocked in blocking solution (2% BSA in PBS) and incubated with indicated antibody overnight in cold and then washed three times with ice-cold PBS. Cells were incubated with FITC-conjugated secondary antibody for 30 min. Nuclei were then fluorescently labeled with DAPI. After washing four times with ice-cold PBS, coverslips were mounted on glass slides. Stained cell were viewed on a confocal imaging system.

2.7. RNA isolation and real-time PCR

Quantitative RT-PCR was performed using real-time PCR with the SYBR Green reporter. Total RNA was extracted from cultured HDFs using TRIZOL reagent (Invitrogen). RNA yield was determined with OD260 nm. Total RNA was extracted and reverse transcribed to cDNAs by Superscript II reverse transcriptase (Invitrogen). Quantitative RT-PCR was performed after stabilizing the RNA. The kit used for RT-PCR was a SYBR Green PCR master kit (Invitrogen), which were optimized to the desired concentration. Each sample was tested three times. The primers used for this experiment were purchased from BIONEER (P282659)

2.8. RNA interference

The transfection of siRNA duplexes was performed as described previously [13]. Briefly, senescent HDFs (5×10^4) were plated in a 100 mm dish, transfected with 0.5 nM siRNA and oligofectamine™ reagent in serum-free medium and incubated for 4 h at 37 °C in a CO_2 incubator. Following incubation, the cells were supplied with growth medium containing 10% fetal bovine serum. The specific siRNA for Nup107 was purchased from BIONEER Co.

3. Results

3.1. Decreased expression of Nup107 in aged cells and organs

We previously found a decrease in the expression of Nup107 in senescent cells using microarray analysis [14]. These results were confirmed using a real-time PCR (Fig. 1A) and Western blotting (Fig. 1B). The expression of Nup107 in young HDFs was 4- to 5-fold higher to that in senescent HDFs (Fig. 1C). And Western blot analysis showed the lower levels of Nup107 in tissues of liver, lung and intestine tissues from the aged mice (Fig. 1D).

3.2. Effect of Nup107 depletion on cellular proliferation

To explore the functional consequence of Nup107 depletion in young HDFs, we evaluated the effect of Nup107-specific siRNA

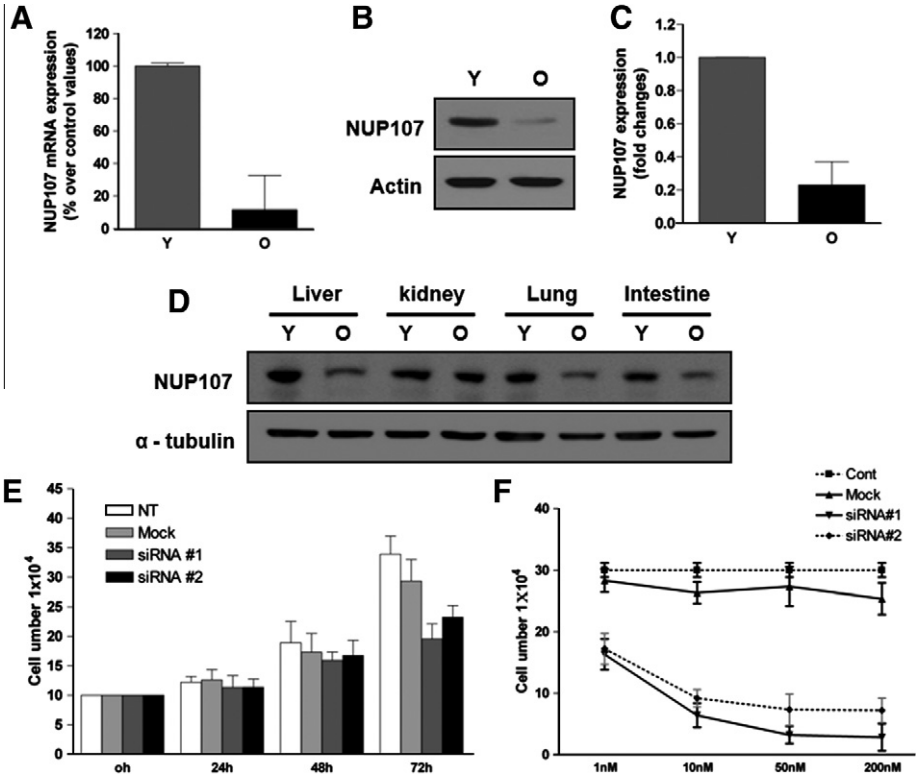

Fig. 1. Nup107 expression is decreased in senescent human diploid fibroblasts (HDFs) and older tissues. (A) Decreased expression of mRNAs encoding proteins involved in nucleocytoplasmic trafficking in senescent HDFs. Total RNA was extracted from young (Y) and senescent (O) fibroblasts, and analyzed by real-time PCR for Nup107 mRNA expression. (B) Measurement of Nup107 protein expression using anti-Nup107 antibody. (C) Quantified Nup107 protein expression levels. Data are means and standard error of three independent experiments. (D) Expression of Nup107 in tissues from young (Y) and old (O) mice. Tissues were obtained as described in Section 2. (E) Depletion of Nup107 using siRNA inhibits the proliferation of HDF cells. Kinetic analysis of the responses of HDFs to Nup107-specific siRNAs. HDFs were transfected with siRNA1, siRNA2, or mock siRNA. Cell numbers were counted at the indicated time points. The data are mean ± SEM of three independent experiments. (F) Dose effects of siRNA. HDF cells were incubated with the indicated concentrations of Nup107 siRNA1 or mock siRNA for 72 h. Cell numbers were counted. The data are mean ± SEM of three independent experiments.

treatment on HDF proliferation. As shown in Supplementary Fig. 1, all three siRNAs tested downregulated Nup107 expression in young HDFs. We next analyzed the antiproliferative effect of Nup107 siRNA on HDF cells at different time points. Compared with control cells, Nup107-knockdown cells displayed significantly reduced proliferation in a direct cell count assay (Fig. 1E). Transfection with siRNA1 or siRNA2 reduced the average cell number by 36% or 23%, respectively, at 72 h. At this time point, no cell death was detected by microscopic analysis. To examine the dose-kinetics of this antiproliferative effect, we treated HDFs with different concentrations of siRNA1 for 72 h. As shown in Fig. 1F, the proliferation of HDFs was reduced nearly 36% with transfection at 1 nM siRNA1 and almost maximally inhibited with transfection at 50 nM siRNA1

3.3. Effect of Nup107 depletion on nuclear translocation of p-ERK after EGF treatment

Owing to its strong inhibitory effect, as demonstrated in Western blot analysis, siRNA1 was used further to examine the impact of Nup107 knockdown on the nuclear translocation of p-ERK. We analyzed the EGF-induced distribution of p-ERK in young HDFs transfected with siRNA1. As shown Fig. 2A and B, p-ERK1/2 did not efficiently translocate to the nucleus in NUP107-knockdown cells following EGF treatment, but instead accumulated in the cytoplasm. These findings were confirmed by immunocytochemical analysis of HDF cells (Fig. 2C). These results mirror the similar defects in nuclear trafficking in senescent cells [9].

3.4. Effect of Nup107 depletion on Elk phosphorylation and c-Fos expression in EGF-treated cell

We next examined downstream effectors of ERK signaling in senescent HDFs. Phosphorylation of Elk-1 as a result of the activation of the MEK/ERK pathway is necessary for c-Fos gene activation [1–5]. We observed the reduced Elk-1 phosphorylation on Ser383 (the target for phosphorylation by ERK) in response to EGF (Fig. 3A) and markedly decreased induction of c-Fos mRNA in senescent fibroblasts (Fig. 3C, Left panel). These findings are consistent with the results of previous studies of ERK signaling in senescent cells. To investigate whether the knockdown of Nup107 affects downstream ERK signaling, we analyzed p-Elk protein levels and c-Fos mRNA levels in Nup107-knockdown cells after EGF stimulation. The level of Elk (Ser383) phosphorylation was significantly lower in Nup107-knockdown cells than in control cells (Fig. 3B). The downregulation of Nup107 also reduced c-Fos mRNA expression (Fig. 3C, Right panel). The dysfunction of ERK signaling in Nup107-knockdown cells closely resembles the similar impairment in senescent cells.

3.5. Effect of Nup107 depletion on cancer cell proliferation

An analysis of published gene expression data using Oncomine [15] revealed that Nup107 mRNA expression is increased in anaplastic oligodendroglioma (Supplementary Fig. 2). As we were interested in investigating the role of Nup107 in this cancer cells (SNU-738 cell line), we transfected the cancer cells with Nup107-specific siRNA and then examined cell proliferation. A direct cell

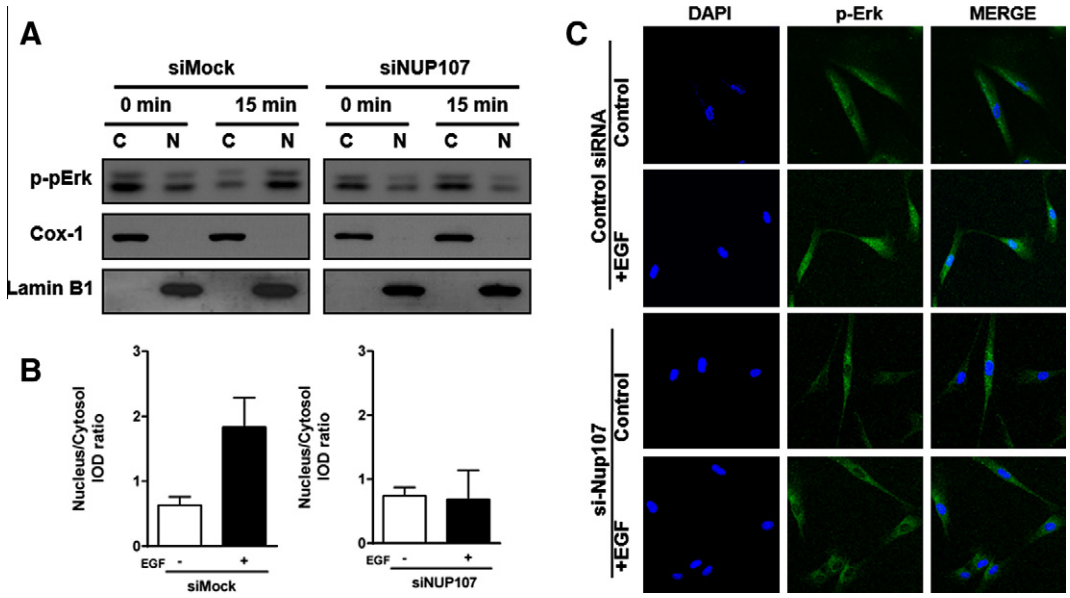

Fig. 2. Depletion of Nup107 results in impaired nuclear translocation of p-ERK. (A) After treatment with 10 ng/ml EGF for 15 min, equal amounts of cytoplasmic and nuclear lysates from young (left) and senescent (right) HDFs were subjected to immunoblot analysis using anti-p-ERK antibody. Cox-1 and lamin B1 was used as a cytosolic and nuclear marker respectively (B) quantified nucleus/cytosol integrated optical density (IOD) ratio. Data are means and standard error of three independent experiments (C) HDFs transfected with Nup107-specific or control siRNA were incubated with 10 ng/ml EGF for 15 min. Fixed cells were analyzed by immunofluorescence microscopy performed using FITC-labeled p-Erk-specific antibodies. DNA was stained with DAPI.

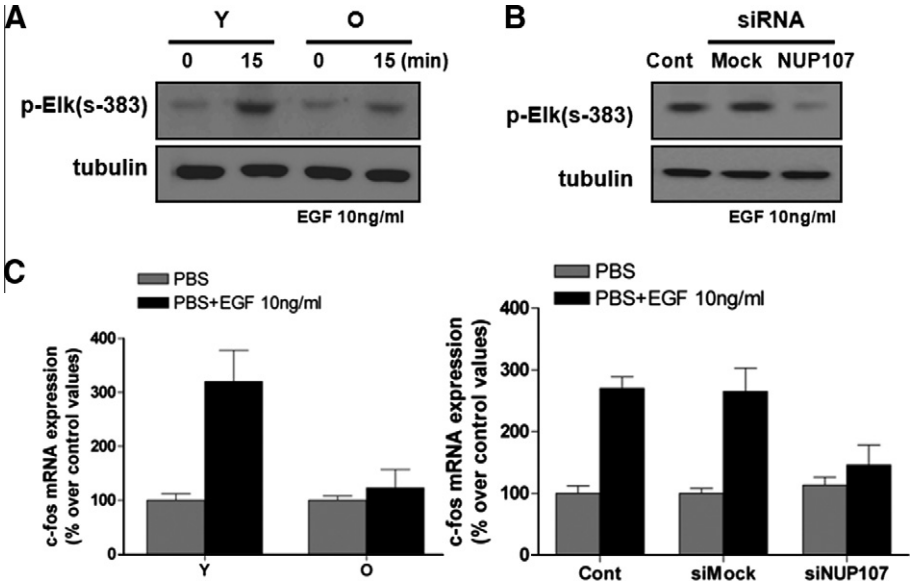

Fig. 3. Dysfunction of ERK downstream signaling in Nup107-knockdown cells. (A) Young (Y) and senescent (O) cells were incubated with 10 ng/ml EGF for 15 min, and then p-Elk protein was analyzed by immunoblotting performed using anti-phospho-Elk (Ser383) antibody. (B) Young HDFs transfected with Nup107-specific or control siRNA were incubated with 10 ng/ml EGF for 15 min, and then p-Elk protein was analyzed by immunoblotting performed using anti-phospho-Elk (Ser383) antibody. (C) c-Fos mRNA expression was analyzed by quantitative real-time RT-PCR. Y: young, O: senescent cells.

count assay demonstrated the reduced proliferation of siRNA-transfected cells compared with untreated control SNU-738 cells. Compared with transfection of control siRNA, siRNA1 or siRNA2 transfection reduced the average cell number by 55 or 37% at 48 h. At 72 h, no viable siRNA1-transfected SNU-738 cells remained, although 51% of siRNA1-transfected SNU-738 cells remained viable (Fig. 4).

4. Discussion

Many signaling molecules and transcription factors must be imported into the nucleus to exert their effects. We have reported the aging-dependent accumulation of p-ERK1/2, actin and gelsolin in the nuclei [9,16] and the lower expression of genes linked to nucleocytoplasmic trafficking in senescent cells compared with that in young cells [10]. These evidences collectively implicate the existence of a functional barrier for nucleocytoplasmic trafficking of the signals in senescent cells.

As mediators of nucleocytoplasmic transport, NPCs are the largest protein assemblies in eukaryotic cells [17,18]. Mammalian NPCs are formed from at least 47 Nups and Nup-associated proteins [19]. Nup107 is the mammalian homolog of yeast Nup84p. The heterooligomeric Nup107 complex, whose components (Nup107, Nup133, Nup96, Nup160, and Sec13) are homologous

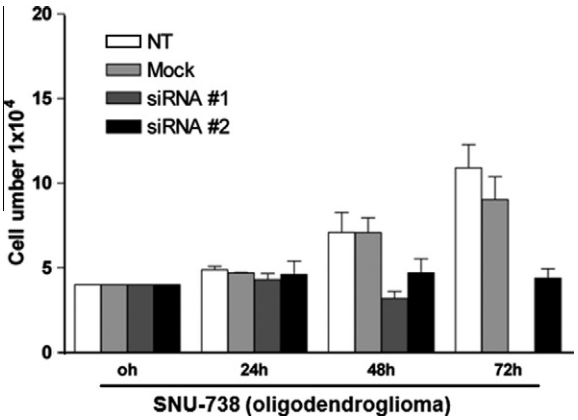

Fig. 4. Depletion of Nup107 using siRNA inhibits cell proliferation of oligodendroglioma (SNU-738) cells. Kinetic analysis of the response of SNU-738 cells. SNU-738 cells were transfected with siRNA1, siRNA2 or mock siRNA. Direct cell numbers were counted at the indicated time points. The data are mean ± SEM of three independent experiments.

to the components of the yeast Nup84p sub-complex, was isolated through dissociation of NPCs [20,21]. Nup107 is a key scaffolding molecule for NPC assembly. Its depletion causes reduction of various nucleoporins and the resultingly defective NPC assembly [16]. We confirmed the effects of Nup107 depletion on other nucleoporins using siRNA (data not shown).

In the present study, it is confirmed that Nup107 expression is markedly decreased in senescent HDFs as well as in aged tissues (Fig. 1). Furthermore, nuclear translocation of active ERK1/2 in response to EGF was impaired in Nup107-depleted HDFs (Fig. 2A–C). These results suggest that the loss of Nup107 would create a functional barrier to the nucleocytoplasmic trafficking of active ERK.

The lack of Elk-1 phosphorylation in senescent cells could be traced to the reduced nuclear translocation of active ERK protein. Although the molecular mechanism regulating the nuclear translocation of ERK is not fully understood, several models have been proposed. For examples, ERK1/2 enters the nucleus through the NPCs via a carrier-independent and energy-independent mechanism [10,11]. Phosphorylated proteins may also enter the nucleus, perhaps by passive diffusion of a monomer or active transport of a dimer [12,13]. ERK1/2 nucleocytoplasmic distribution is also dependent on its nuclear efflux mechanism [14]. ERK can bind nuclear carrier proteins to translocate into the nucleus [15]. In the present study, we used Nup107 siRNA to demonstrate that the nuclear trafficking of p-ERK is partly NPC-dependent (Fig. 2A–C). We also showed that depletion of Nup107 affects downstream effectors of ERK signaling, resulting in decreased Elk phosphorylation and decreased induction of c-Fos gene expression (Fig. 3B and C). These results strongly suggest that impaired ERK signaling in senescent cells stems in part from dysfunctional NPC-dependent nuclear trafficking.

Nucleoporins are overexpressed in many types of cancer, including the breast, colon, and prostrate cancers, and in various cancer cell lines, indicating that it may play a role in cell signaling and survival [22]. Nucleoporin expression is increased during cell division and high in continuously dividing cancer cells. Our analysis of published gene expression data using Oncomine [15] shows that the expression of Nup107 mRNA is increased in cervical cancer, seminoma, and oligodendroglioma, as well as in rectal and colon cancer (data not shown). In the present study, it has been shown that the simple depletion of Nup107 in anaplastic oligodendroglioma cells leads to cell death, which was not observed in normal human diploid fibroblasts (Fig. 4). These findings implicate that cancer cell might be more sensitive than normal cells in regulation of nucleocytoplasmic trafficking, which heralds the novel cancer therapeutic approach by manipulating the nucleocytoplasmic trafficking. Whether the observed cell death was caused by apoptosis or necrosis, and whether it was caspase-dependent or -independent, requires further investigation.

Taken together, these results suggest that senescence-linked hypo-responsiveness to growth factor stimulation may be attributable in part to dysfunctional nuclear trafficking caused by reduced Nup107 expression and that loss of Nup107 may play an important role in the decline of intracellular signaling in senescent cells. These results reveal a novel role of Nup107 in cellular aging and may help in the development of new strategies for control of aging process, as well as for anti-cancer therapy.

Acknowledgments

This work was supported by grants from the National Research Foundation (NRF) through the Ageing and Apoptosis Research Center at Seoul National University (RII-2002-097-08001-0) and The Research Programs of Dual Regulation of Aging and Cancer Project.

Appendix A. Supplementary data

Supplementary data associated with this article can be found, in the online version, at doi:10.1016/j.bbrc.2010.09.025.

References

[1] P.W. Atadja, K.F. Stringer, K.T. Riabowol, Loss of serum response element-binding activity and hyperphosphorylation of serum response factor during cellular aging, Mol. Cell Biol. 14 (1994) 4991–4999.
[2] P. Cohen, The search for physiological substrates of MAP and SAP kinases in mammalian cells, Trends Cell. Biol. 7 (1997) 353–361.
[3] R. Janknecht, W.H. Ernst, V. Pingoud, A. Nordheim, Activation of ternary complex factor Elk-1 by MAP kinases, EMBO J. 12 (1993) 5097–5104.
[4] M.A. Price, F.H. Cruzalegui, R. Treisman, The p38 and ERK MAP kinase pathways cooperate to activate ternary complex factors and c-fos transcription in response to UV light, EMBO J. 15 (1996) 6552–6563.
[5] R. Seger, E.G. Krebs, The MAPK signaling cascade, FASEB J. 9 (1995) 726–735.
[6] M. Tresini, A. Lorenzini, L. Frisoni, R.G. Allen, V.J. Cristofalo, Lack of Elk-1 phosphorylation and dysregulation of the extracellular regulated kinase signaling pathway in senescent human fibroblast, Exp. Cell Res. 269 (2001) 287–300.
[7] T. Seshadri, J. Campisi, Repression of c-fos transcription and an altered genetic program in senescent human fibroblasts, Science 247 (1990) 205–209.
[8] B.P. Keogh, M. Tresini, V.J. Cristofalo, R.G. Allen, Effects of cellular aging on the induction of c-fos by antioxidant treatments, Mech. Ageing Dev. 86 (1996) 151–160.
[9] I.K. Lim, K. Won Hong, I.H. Kwak, G. Yoon, S.C. Park, Cytoplasmic retention of p-Erk1/2 and nuclear accumulation of actin proteins during cellular senescence in human diploid fibroblasts, Mech. Ageing Dev. 119 (2000) 113–130.
[10] S.Y. Kim, S.J. Ryu, H.J. Ahn, H.R. Choi, H.T. Kang, S.C. Park, Senescence-related functional nuclear barrier by down-regulation of nucleo-cytoplasmic trafficking gene expression, Biochem. Biophys. Res. Commun. 391 (2010) 28–32.
[11] T.C. Walther, A. Alves, H. Pickersgill, I. Loiodice, M. Hetzer, V. Galy, B.B. Hulsmann, T. Kocher, M. Wilm, T. Allen, I.W. Mattaj, V. Doye, The conserved Nup107-160 complex is critical for nuclear pore complex assembly, Cell 113 (2003) 195–206.
[12] G.P. Dimri, X. Lee, G. Basile, M. Acosta, G. Scott, C. Roskelley, E.E. Medrano, M. Linskens, I. Rubelj, O. Pereira-Smith, et al., A biomarker that identifies senescent human cells in culture and in aging skin in vivo, Proc. Natl. Acad. Sci. USA 92 (1995) 9363–9367.
[13] S.M. Elbashir, J. Harborth, W. Lendeckel, A. Yalcin, K. Weber, T. Tuschl, Duplexes of 21-nucleotide RNAs mediate RNA interference in cultured mammalian cells, Nature 411 (2001) 494–498.
[14] M.S. Jung, D.H. Jin, H.D. Chae, S. Kang, S.C. Kim, Y.J. Bang, T.S. Choi, K.S. Choi, D.Y. Shin, Bcl-xL and E1B-19K proteins inhibit p53-induced irreversible growth arrest and senescence by preventing reactive oxygen species-dependent p38 activation, J. Biol. Chem. 279 (2004) 17765–17771.
[15] D.R. Rhodes, J. Yu, K. Shanker, N. Deshpande, R. Varambally, D. Ghosh, T. Barrette, A. Pandey, A.M. Chinnaiyan, Oncomine: a cancer microarray database and integrated data-mining platform, Neoplasia 6 (2004) 1–6.
[16] J.S. Ahn, I.S. Jang, J.H. Rhim, K. Kim, E.J. Yeo, S.C. Park, Gelsolin for senescence-associated resistance to apoptosis, Ann. NY Acad. Sci. 1010 (2003) 493–495.

[17] T.D. Allen, J.M. Cronshaw, S. Bagley, E. Kiseleva, M.W. Goldberg, The nuclear pore complex: mediator of translocation between nucleus and cytoplasm, J. Cell Sci. 113 (Pt 10) (2000) 1651–1659.
[18] K.J. Ryan, S.R. Wente, The nuclear pore complex: a protein machine bridging the nucleus and cytoplasm, Curr. Opin. Cell Biol. 12 (2000) 361–371.
[19] M. Platani, R. Santarella-Mellwig, M. Posch, R. Walczak, J.R. Swedlow, I.W. Mattaj, The Nup107-160 nucleoporin complex promotes mitotic events via control of the localization state of the chromosome passenger complex, Mol. Biol. Cell 20 (2009) 5260–5275.
[20] A.M. Copeland, W.W. Newcomb, J.C. Brown, Herpes simplex virus replication: roles of viral proteins and nucleoporins in capsid–nucleus attachment, J. Virol. 83 (2009) 1660–1668.
[21] S. Otsuka, S. Iwasaka, Y. Yoneda, K. Takeyasu, S.H. Yoshimura, Individual binding pockets of importin-beta for FG-nucleoporins have different binding properties and different sensitivities to RanGTP, Proc. Natl. Acad. Sci. USA 105 (2008) 16101–16106.
[22] S. Xu, M.A. Powers, Nuclear pore proteins and cancer, Semin. Cell Dev. Biol. 20 (2009) 620–630.